



Published in final edited form as:

J Alzheimers Dis. 2020 ; 76(3): 1083–1102. doi:10.3233/JAD-200436.

Effects of probiotic supplementation on short chain fatty acids in the *App^{NL-G-F}* mouse model of Alzheimer's disease

Harpreet Kaur^a, Svetlana Golovko^a, Mikhail Y. Golovko^a, Surjeet Singh^b, Diane C. Darland^c, Colin K. Combs^a

^aDepartment of Biomedical Sciences, University of North Dakota, School of Medicine and Health Sciences, 1301 N Columbia Road, Grand Forks, ND 58202-9037

^bDepartment of Neuroscience, Canadian Centre for Behavioural Neuroscience (CCBN), University of Lethbridge, 4401 University Drive, Lethbridge, AB, T1K 3M4, Canada

^cDepartment of Biology, University of North Dakota, College of Arts & Sciences, 10 Cornell Street, Grand Forks, ND 58202-9019

Abstract

Background: The intestinal microbiota and its metabolites, particularly short-chain fatty acids (SCFAs), have been implicated in immune function, host metabolism, and even behavior.

Objective: This study was performed to investigate whether probiotic administration influences levels of intestinal microbiota and their metabolites in a fashion that may attenuate brain changes in a mouse model of Alzheimer's disease (AD).

Methods: C57BL/6 wild-type (WT) mice were compared to *App^{NL-G-F}* mice. The animals were treated with either vehicle or probiotic (VSL#3) for 8 weeks. Fecal microbiome analysis along with A β , GFAP, Iba-1, c-Fos, and Ki-67 immunohistochemistry was done. SCFAs were analyzed in serum and brains using UPLC-MS/MS.

Results: Probiotic (VSL#3) supplementation for 2 months resulted in altered microbiota in both WT and *App^{NL-G-F}* mice. An increase in serum SCFAs acetate, butyrate and lactate were found in both genotypes following VSL#3 treatment. Propionate and isobutyrate were only increased in *App^{NL-G-F}* mice. Surprisingly, VSL#3 only increased lactate and acetate in brains of *App^{NL-G-F}* mice. No significant differences were observed between vehicle and VSL#3 fed *App^{NL-G-F}* hippocampal immunoreactivities of A β , GFAP, Iba-1 and Ki-67. However, increased hippocampal c-Fos staining increased in VSL#3 fed *App^{NL-G-F}* mice.

Conclusion: These data demonstrate intestinal dysbiosis in the *App^{NL-G-F}* mouse model of AD. Probiotic VSL#3 feeding altered both serum and brain levels of lactate and acetate in *App^{NL-G-F}* mice correlating with increased expression of the neuronal activity marker, c-Fos.

^{*}Corresponding author: Colin K. Combs, PhD, University of North Dakota, School of Medicine and Health Sciences, Department of Biomedical Sciences, 1301 N Columbia Road, Suite W315, Grand Forks, ND 58202-9037, +1 701 777-4025 colin.combs@und.edu.

CONFLICT OF INTEREST

The authors have no conflict of interest to report.

Keywords

Alzheimer disease; microbiota; probiotics; butyrate; plaques; gliosis; short chain fatty acids

INTRODUCTION

Alzheimer's disease (AD) is a neurodegenerative condition hypothesized to develop due to dysfunction of two major proteins, amyloid beta ($A\beta$) and microtubule-associated protein, tau [1]. Multiple factors are suggested to contribute to the etiology of AD including, but not limited to, aging, genetics, head injury, and exposure to certain chemicals, compounds, and metals including iron, cadmium etc. [2–4]. Recent evidence supports a positive connection between Alzheimer's disease (AD) and gut microbiota [5, 6]. The cellular milieu in the gut includes the microbiota, which refers to the bacteria, viruses, and fungi. Changes in gut microbial composition have been found in AD patients that correlate with the levels of certain AD biomarkers in cerebrospinal fluid. These results support a role for the health of the gastrointestinal tract and the enteric nervous system (ENS) in the pathophysiology of AD [7–9].

The intestinal microbiota not only plays an important part in digestion but also supports overall homeostasis by influencing metabolism, growth, development, immune function, and protection from pathogens [10–12]. A number of factors can affect the intestinal microbiota composition such as dietary changes, antibiotic exposure, and infection leading to the loss of bacterial homeostasis implicated in gastrointestinal and neurological disorders [13, 14]. Recent studies continue to address how microbial metabolism may influence health outcomes associated with extra-intestinal disorders including allergy, metabolic syndrome, cardiovascular disease, and obesity [15–17]. However, the mechanisms by which specific microbes and their metabolites contribute to disease prevention or progression remain largely unknown.

It has been demonstrated that intestinal microbes can affect several host metabolic pathways, many of which are involved with carbohydrate or amino acid metabolism [18]. Short chain fatty acids (SCFAs) are a primary class of signaling molecules including iso-butyric acid and butyric acid (C4), propionic acid (C3), acetic acid (C2), and formic acid (C1) that are produced by intestinal bacteria during metabolism of dietary carbohydrates and fibers in the colon [19–21]. There is a scarcity of data describing whether, and how, intestinal bacteria derived SCFA metabolites influence the brain in AD.

Therefore, this study was performed to investigate the role of intestinal microbiota and their metabolites, specifically SCFAs, on AD pathology using the *App*^{NL-G-F} mouse model of disease. To understand this, we manipulated the gut bacteria using probiotic, VSL#3, which is a combination of eight different lactic acid producing bacteria. We hypothesized that a disease or probiotic-associated shift in intestinal microbiota might result in a corresponding shift in levels of bacterial metabolic products, e.g. SCFA, that could influence the presentation of disease in the brain.

Our data supports the idea that the intestinal microbiota is altered during AD resulting in a change in serum and brain SCFA metabolite levels in the AD mice. Moreover, modulating the intestinal microbiota using a probiotic feeding paradigm altered select SCFA levels correlating with a marker of neuronal activity in the brain.

MATERIALS AND METHODS

Animals

App^{NL-G-F} mice were obtained from Dr. Takaomi C. Saido, Laboratory for Proteolytic Neuroscience, RIKEN Center for Brain Science, Japan. These mice were selected for use as these mice do not overexpress APP and expression is under endogenous promoter control. However, A β is elevated due to the combined effects of three mutations associated with familial AD. An APP construct containing a humanized A β region, includes the Swedish “NL”, the Iberian “F”, and the Arctic “G” mutations was used [22]. Fifteen female *App^{NL-G-F}* and 15 C57BL/6 (wild type) control mice were used at 6–8 months of age. Both genotypes were bred and housed under the same conditions (animal facility, room, food, and water) to avoid potential artifacts due to the environment (bedding, diet, lighting etc.) that are relevant in microbiome studies. Mice were weaned and used at 6–8 months age to ensure acclimation to the environment at the start of the treatment regimen. Animal use was approved by the University of North Dakota Institutional Animal Care and Use Committee (IACUC) protocol. The animals were provided food and water *ad libitum* and housed in a specific pathogen-free room with a 12-h light/dark cycle.

Animal groups and probiotic (VSL#3) dosing

Animals were randomly assigned into four groups: 1) wild type supplemented with vehicle (WT Vehicle), 2) wild type supplemented with VSL#3 (WT VSL), 3) *App^{NL-G-F}* supplemented with vehicle (*App^{NL-G-F}* Vehicle), and 4) *App^{NL-G-F}* supplemented with VSL#3 (*App^{NL-G-F}* VSL#3). The vehicle used was MediGel® (Clear H₂O, Portland, ME, USA) and VSL#3 was dissolved in the vehicle and administered to animals daily at estimated mean water consumption of 5 mL/25g mouse/day. The treatment was given for eight weeks and the dose of probiotic VSL#3 (0.32×10^9 CFU bacteria/25g mice) was calculated based on the body surface area normalization method from the recommended human dose of VSL#3 [23]. VSL#3 is a commercially available probiotic cocktail (Leadiant Biosciences, Inc., Gaithersburg, MD, USA) of eight strains of lactic acid-producing bacteria: *Lactobacillus plantarum*, *Lactobacillus delbrueckii subsp. Bulgaricus*, *Lactobacillus paracasei*, *Lactobacillus acidophilus*, *Bifidobacterium breve*, *Bifidobacterium longum*, *Bifidobacterium infantis*, and *Streptococcus salivarius subspecies, thermophilus*. VSL#3 is a well-known medical food that has been shown to improve disease symptoms in the treatment of ulcerative colitis and pouchitis, an inflammation of the ileal pouch in colectomy patients, liver cirrhosis and hepatic encephalopathy [24, 25].

Antibodies and reagents

Antibodies against GFAP and amyloid beta (A β) were purchased from Cell Signaling Technology Inc. (Danvers, MA, USA). Anti-c-Fos antibody was purchased from Abcam (Cambridge, MA, USA). Anti-Iba-1 antibody was purchased from Wako Chemicals USA,

Inc. (Richmond, VA, USA). Elite Vectastain ABC reagents, Vector VIP, biotinylated anti-rabbit, and anti-mouse antibodies were purchased from Vector Laboratories Inc (Burlingame, CA, USA). The A β 1–40 and A β 1–42 enzyme-linked immunosorbent assay (ELISA) kits were obtained from EMD Millipore (Burlington, MA). Standards used in mass spectroscopy analysis were purchased from Millipore-Sigma Burlington, MA, USA. Autosampler vials were obtained from ThermoFisher Scientific, (Waltham, MA, USA), Silanized micro-vial inserts from Agilent (Santa Clara CA; part #5181–8872) and inserts were from VWR (Radnor, PA, USA).

Fecal sample collection and microbiome analysis

After 8 weeks of probiotic feeding, fecal samples were obtained by placing each mouse separately in a clean cage for 10–30 min and fecal pellets were collected in a sterile 1.5 mL Eppendorf tube. More than 90% of the mice excreted a fecal pellet within one min of being placed into a clean cage. In those instances, in which a mouse did not pass stool within 30 mins, the mouse was gently picked up vertically by the tail for 20–30 seconds until a stool pellet was excreted and collected. Samples were stored at 4°C until all samples were collected and later stored at –80°C until microbiome analysis. The fecal samples were sent to RTL Genomics (Research and Testing Laboratory, Lubbock, TX, USA) for 16S rRNA sequencing. Hypervariable regions V1 to V3 of 16S rRNA gene were amplified for sequencing at RTL Genomics in a reaction using HotStarTaq Master Mix Kit (Qiagen, Inc., Germantown, MD, USA) with the universal primer set 27F/519R.

Short chain fatty acid analysis

Carboxylic acids moiety of SCFAs were analyzed as nitrophenyl hydrazide derivatives (CANPD). Proteins from serum (10 μ L) and hippocampus (10 mg) were precipitated after sonication with 280 μ L of methanol containing butyrate-¹³C₄, propionate-¹³C₃, and lactate-¹³C₃ (20 ng each) as internal standards. After centrifugation at 10,000 x g, the supernatant was subjected to derivatization to obtain carboxylic acids nitrophenyl hydrazides as described in [26] with modifications. Because ethanol showed high levels of short chain carboxylic acid contamination, it was substituted with methanol for the derivatization reaction. All reagents for derivatization were from Millipore-Sigma Burlington, MA, USA. Briefly, the supernatant volume was brought up to 300 μ L with methanol, mixed with 300 μ L of pyridine, 300 μ L of 1-ethyl-3-(3-dimethylaminopropyl) carbodiimide (250 mM in methanol), 300 μ L of 2-Nitrophenyl hydrazine hydrochloride (20 mM in methanol), and incubated at 60°C for 20 min. After quenching with 200 μ L of potassium hydroxide (15% in 20% methanol) at 60°C for 20 min, 3 mL of Phosphoric acid (0.5 mM in water) were added to each sample. CANPD were extracted with 4 mL of ether and the extract was washed with 4 mL of water. Centrifugation at 1,500 x g was used to separate phases during extraction and washing steps.

An LC-MS method was used for CANPD quantification. CANPD extracts were evaporated under nitrogen stream, transferred to silanized microvial inserts (Agilent, Santa Clara CA; part #5181–8872) with 100 μ L of ether, evaporated, re-dissolved in 20 μ L of 50% methanol in water, and 10 μ L was analyzed on UPLC-MS/MS in the selected ion monitoring mode.

UPLC separation was performed on a Waters ACUITY UPLC HSS T3 column (1.8 μM , 100 \AA pore diameter, 2.1 \times 150mm, Waters, Milford, MA) with an ACUITY UPLC HSS T3 precolumn (1.8 μM , 100 \AA pore diameter, 2.1 \times 5mm, Waters) at a temperature of 55 $^{\circ}\text{C}$ using a previously described method [2, 3]. The LC system consisted of a Waters ACUITY UPLC pump with a well plate autosampler at 8 $^{\circ}\text{C}$. Solvent A was water containing 0.1% formic acid and solvent B was acetonitrile with 0.1% formic acid. The flow rate was maintained at 0.45 mL/min. CANPD were eluted with increasing gradient of solvent B from 39% to 98% as we previously described [27]. A quadrupole time-of-flight mass spectrometer (Q-TOF, Synapt G2-S, Waters) was used for detection as described previously [28]. The electrospray ionization was set in negative ion mode with the cone voltage at 20 V, and the capillary voltage at 1.51 kV. The source and desolvation temperatures were 110 $^{\circ}\text{C}$ and 350 $^{\circ}\text{C}$, respectively. MSE mode was used to collect data. Leucine enkephalin (400 pg/ μL in ACN: water, 50:50 by volume) was used for mass correction. MassLynx V4.1 software (Waters) was used for instrument control, acquisition, and sample analysis. Nitrophenyl hydrazide derivatives of acetate ($m/z=194.0566$), and propionate ($m/z=208.0722$) were quantified against propionate-13C3, ($m/z=211.0823$), lactate ($m/z=224.0671$) and pyruvate ($m/z=222.0515$) were quantified against lactate-13C3, ($m/z=227.0772$), and butyrate and isobutyrate ($m/z=222.0879$) - against butyrate-13C4 ($m/z=226.1013$).

Ki-67 stereology and counting in hippocampus

Immunopositive Ki-67 nuclei were counted in the subventricular zone (SVZ) using an Olympus BX51WI microscope with a motorized XYZ stage. Unbiased quantification of nuclei was conducted using the optional fractionator workflow in StereoInvestigator 11.0 (MicroBrightfield, Inc., Wiliston, VT). For cell counting, a tight contour was outlined around the subventricular zone at the same region for all the treatment conditions. Positive nuclei were counted in every 24th section in systematically selected frames based on an optical dissector frame (50 \times 50 μm) and a grid size (125 \times 125 μm) that were empirically determined by initial oversampling. The section thickness was measured at each sampling site. The sampling and counting paradigm resulted in a Coefficient of Error (CE) less than 0.1 (10%) for all samples counted. The total numbers were estimated in StereoInvestigator with the optical fractionator formula ($N=1/ssf.1/asf.1/hsf.\Sigma Q-$) where ssf =section sampling fraction (10), asf =area sampling fraction (area sampled/total area), hsf =height sampling fraction (counting frame height/30 μm), and $\Sigma Q-$ (total particle count). Four sections (40 μm) per brain were used at a counting interval of every 24th section and 7 brains were quantified per treatment condition. Cells in the dentate gyrus (DG) were counted manually due to the few Ki-67 positive cells being present in hippocampus.

Immunohistochemistry

Following the eight-week treatment paradigm the left brain hemisphere of each animal was fixed in 4% paraformaldehyde and prepared for histologic analysis as described previously [29]. Briefly, paraformaldehyde-fixed tissue was embedded in a 15% gelatin (in 0.1 M phosphate buffer) matrix and immersed in a 4% paraformaldehyde for 2 days to harden the gelatin matrix followed by two changes of 30% sucrose for cryoprotection for two days each. The blocks were then flash frozen using dry ice/isomethylpentane, and 40 μm serial sections were cut using a freezing microtome. Serial sections of 40 μm were stored at 4 $^{\circ}\text{C}$ in

PBS with 0.1% sodium azide until immunostaining was performed. Anti-A β (1:1000), anti-GFAP (1:700), anti-Iba-1 (1:750), anti-cFos (1:2000) and anti-Ki-67 (1:500, used sodium citrate, heat mediated antigen retrieval) antibodies were used for immunodetection in sections followed by incubation with biotinylated secondary antibodies (1:2000 dilution; Vector Laboratories) and an avidin/biotin complex (Vector ABC kit). Immunoreactivity was visualized using Vector VIP as the chromogen. The stained sections were mounted onto gelatin-coated slides and cover slipped using Permount (Vector Laboratories) following a standard dehydrating procedure through a series of ethanol concentrations and Histo-Clear (National Diagnostics, Atlanta, GA, USA). A Leica DM1000 microscope and Leica DF320 digital camera system (Leica Microsystems Inc., Buffalo Grove, IL, USA) were used to take images and quantification of immunostaining was performed as described previously [30]. Briefly, optical densities from serial hippocampus sections from each condition were measured using Adobe Photoshop software (Adobe Systems). The average values for each condition were analyzed and plotted. This entailed 2 hippocampus sections per brain, 7 brains per condition or 14 sections from each condition that were used for immunohistochemistry analysis.

Enzyme linked immunosorbent assay (ELISA) for Amyloid- β

Following the eight-weeks treatment paradigm, the animals were euthanized via CO₂ asphyxiation followed by cervical dislocation and cardiac exsanguination. The hippocampi of each animal were collected for biochemical procedures. The right hippocampus of each animal was collected, flash frozen in liquid nitrogen, and stored at -80 °C for subsequent use. A small part of the hippocampus was weighed and lysed in ice cold radioimmunoprecipitation assay buffer (RIPA) buffer (20 mM Tris, pH 7.4, 150 mM sodium chloride (NaCl), 1 mM Sodium orthovanadate (Na₃VO₄), 10mM Sodium fluoride, 1 mM ethylenediaminetetraacetic acid (EDTA), 1 mM (ethylene glycol-bis(β -aminoethyl ether)-N,N,N',N'-tetraacetic acid) EGTA, 0.2 mM phenylmethylsulfonyl fluoride, 1% Triton, 0.1% sodium dodecyl sulfate (SDS), and 0.5% deoxycholate) with protease inhibitors (4-(2-aminoethyl)benzenesulfonyl fluoride hydrochloride 1 mM, aprotinin 0.8 μ M, leupeptin 21 μ M, bestatin 36 μ M, pepstatin A 15 μ M, E-64 14 μ M). The samples were mechanically homogenized using beads in a Bullet Blender Storm homogenizer 24 (Next Advance, Inc. Troy, NY, USA) and later centrifuged to remove the insoluble content. The resulting clear tissue lysate (supernatant) was used for soluble A β 1-40 and A β 1-42 ELISAs. The pellet or insoluble content was re-suspended in 5M guanidine HCl/50 mM Tris HCl, pH 8.0 and samples were again bullet blended and centrifuged (21,000 g, 4°C, 10 min) and the supernatant was removed and used to determine insoluble A β concentrations (A β 1-40 and A β 1-42 ELISA). The levels of soluble and insoluble A β 1-40 and A β 1-42 were quantified by using commercially available ELISA kits from MilliporeSigma. The levels of A β 1-40 and A β 1-42 (soluble and insoluble) were reported as pg/mL per mg protein derived from a standard curve established for each protein. Protein concentrations of cell lysates were determined using the bicinchoninic acid (BCA) protein determination assay (ThermoFisher Scientific).

Behavioral analysis

Light-dark box (Stoelting) testing was performed to assess anxiety-like behavior in the mice [31, 32]. The light/dark box consisted of two compartments, light and dark, connected by a door in the middle of the wall that separated the two compartments. Each animal was placed individually in the light compartment and allowed to move freely in the apparatus for 10 min. The movement was recorded and analyzed by Anymaze software (Stoelting Co., Wood Dale, IL). The total number of entries into the dark and light chamber, the total time spent in the light chamber (percentage of time spent in light) and latency to first enter the dark compartment were examined. After each trial, the chambers were cleaned, and the next mouse was placed for testing.

Statistical analyses

Statistical analyses were performed using Graphpad Prism (Prism version 7.00 for Windows, GraphPad Software, La Jolla California USA). The tests for outliers (Grubb's test) and normality (Shapiro-Wilk test) were performed on each data set. If the data followed normal distribution a t-test (two tailed) was performed. If the data was not normally distributed, a nonparametric Mann Whitney test was performed to compare the two conditions. All plots in the manuscript were generated using GraphPad software. Results are presented as mean values \pm the standard error of the mean (SEM). Differences were considered significant when $p < 0.05$ and indicated in the figure legend as appropriate.

RESULTS

Probiotic supplementation altered the fecal microbiome of both C57BL/6 (WT) and App^{NL-G-F} mice.

To investigate the existence of gut dysbiosis and the effect of eight weeks of VSL#3 probiotic supplementation in AD mice, fecal samples of WT and App^{NL-G-F} (AD) mice were subjected to 16S rRNA sequencing. The relative abundance results showed a dramatic difference across treatments in control and AD mice (Fig. 1A). App^{NL-G-F} mice had a significant increase in *Clostridia*, *Lachnospiraceae* and *Akkermansia* genera and both an increase and a decrease in order *Bacteroidales* following probiotic treatment (Fig. 1B). While a decrease in *Lachnospiraceae*, *Alistepes*, and *Oscillibacter* was observed in WT mice treated with probiotics (Fig. 1B).

Probiotic supplementation increased serum SCFAs in WT and App^{NL-G-F} mice.

In order to investigate the effect of altered gut bacterial composition on bacterial fermentation end-products, we elected to quantify levels of SCFAs, acetate, butyrate, isobutyrate, lactate and propionate in serum from WT and App^{NL-G-F} mice. We also examined the impact of probiotic supplementation on the concentration of SCFAs in serum. Supplementation with probiotic significantly increased acetate, butyrate, lactate, isobutyrate and propionate in the serum of VSL#3 fed App^{NL-G-F} compared to their vehicle controls (Fig. 2). The dietary response was highly variable between genotypes, as probiotic supplementation increased only acetate and lactate in WT mice (Fig. 2). To understand the association between alterations in serum SCFAs and changes in gut bacteria, a Pearson's

correlation analysis was performed, and the results graphed as a correlation map (Fig. 3A) and as a p value map (Fig. 3B) for comparison. The results showed that an increase in serum propionate in vehicle fed *App^{NL-G-F}* mice correlated with a high abundance of *Clostridia* class bacteria and a low abundance of the *Parasutterella* genus. However, there was no significant correlation between increased other serum SCFAs and any of the bacteria genera. Following probiotic supplementation, the order *Bacteroidales* positively correlated with an increase in serum butyrate and isobutyrate in *App^{NL-G-F}* mice (Fig. 3). A decrease in the genus *Parasutterella* negatively correlated with an increase in acetate in brains of *App^{NL-G-F}* mice treated with probiotics (Fig. 3).

Probiotic supplementation increased hippocampal SCFAs in *App^{NL-G-F}* mice.

The impact of probiotic supplementation on levels of acetate, butyrate, isobutyrate, lactate and propionate were assessed in hippocampi from WT and *App^{NL-G-F}* mice. Surprisingly, probiotic supplementation decreased acetate and propionate SCFAs in wild type mice (Fig. 4). Similar to the serum findings, elevated levels of acetate and lactate were observed in the hippocampi of VSL#3 fed *App^{NL-G-F}* mice (Fig. 4). Correlation analysis was performed comparing fecal bacterial composition and brain SCFAs using Pearson's correlation and graphed as a correlation maps (Fig. 5A) or a p value map (Fig. 5B). The increase in hippocampal acetate positively correlated with the genus *Lactobacillus* and negatively correlated with the genus *Parasutterella* in *App^{NL-G-F}* mice treated with probiotics (Fig. 5). The VSL#3-induced increase in hippocampal acetate levels negatively correlated with class *Clostridia* (Fig. 5).

Probiotic supplementation had no effect on Ki-67 immunoreactivity in *App^{NL-G-F}* mice.

Recently, gut microbiota have been reported to influence neurogenesis in the brain [33]. Using Ki-67 immunoreactivity as a maker of proliferation and a surrogate for possible neurogenesis changes, we investigated whether altered gut microbiota in *App^{NL-G-F}* mice had any effect on neurogenesis in the dentate gyrus and subventricular zone. Although there appeared to be less overall Ki-67 immunoreactivity in *App^{NL-G-F}* dentate gyrus compared to WT, the probiotic supplementation for eight weeks showed no effect on Ki-67 immunoreactivity in either the dentate gyrus or the subventricular zone of *App^{NL-G-F}* or WT mice (Fig. 6).

Probiotic supplementation increased c-Fos immunoreactivity in *App^{NL-G-F}* mice.

As a measure of assessing probiotic supplementation effects on neuronal activity, c-Fos immunostaining was performed on brain sections. c-Fos is commonly used as a functional marker of activity in neurons [34]. Eight weeks of probiotic supplementation resulted in a significant increase in c-Fos immunoreactivity in *App^{NL-G-F}* mice treated with VSL#3 with no change in WT mice (Fig. 7).

Probiotic supplementation had no effect on A β , GFAP, and Iba-1 immunoreactivity in *App^{NL-G-F}* mice.

Since we observed a remarkable difference in serum and brain SCFA levels following probiotic supplementation, we examined whether changes occurred in plaque load and

gliosis in *App^{NL-G-F}* mice. Immunohistochemistry for A β , GFAP, and Iba-1 was performed using brain sections from WT and *App^{NL-G-F}* mice. Surprisingly, probiotic supplementation did not alter microgliosis, astrogliosis or A β plaque load in *App^{NL-G-F}* mice (Fig. 8).

Probiotic feeding had no effect on A β levels in the hippocampus *App^{NL-G-F}* mice.

In order to provide a more quantifiable assessment of brain A β levels, ELISAs were next performed. The levels of A β 1–40 and A β 1–42, both soluble and insoluble, were assessed from the hippocampi of WT and *App^{NL-G-F}* mice. As expected, *App^{NL-G-F}* mice demonstrated high levels of soluble and insoluble A β 1–40 and 1–42 (Fig. 9). However, probiotic supplementation of *App^{NL-G-F}* animals had no effect on A β levels, consistent with our immunolabeling findings (Fig. 9).

Probiotic supplementation altered anxiety-like behavior in *App^{NL-G-F}* mice.

Even though we did not observe a change in plaque load or gliosis in VSL#3 fed *App^{NL-G-F}* mice, the increased c-Fos immunoreactivity and changes in brain SCFA levels demonstrated clear brain effects. Since we previously did not observe probiotic feeding effects on memory in *App^{NL-G-F}* mice, we elected to quantify whether VSL#3 feeding might influence a distinct behavioral dysfunction associated with AD, anxiety. Anxiety-like behavior was quantified using a light-dark apparatus. The total number of entries into the dark chamber, total time spent in the light chamber (percentage of time spent in light) and latency to first enter the dark compartment were examined. VSL#3 supplementation of the *App^{NL-G-F}* mice decreased the number of entries into the dark and normalized the latency to first enter the dark to WT levels demonstrating an anxiolytic effect of the probiotic feeding (Fig. 10).

DISCUSSION

In this study we assessed potential beneficial effects of modulating gut bacteria using the probiotic VSL#3 in an amyloidosis model of AD, *App^{NL-G-F}* mice. We found that VSL#3 had a differential effect in WT and *App^{NL-G-F}* mice which could be due the difference in the microbiota composition between two genotypes. *App^{NL-G-F}* mice had a distinct microbiota when compared to WT mice which was associated with several differences in both serum and brain SCFA concentrations between WT and *App^{NL-G-F}* mice with and without the probiotic supplementation. Probiotic feeding and SCFA changes did not correlate with increased neurogenesis-like proliferation in the *App^{NL-G-F}* mice or alter plaque load or gliosis. However, VSL#3 supplementation significantly increased hippocampal c-Fos staining in *App^{NL-G-F}* mice that correlated with increases in brain lactate and acetate levels and reduced anxiety-like behavior.

Our fecal microbiome analysis revealed comparatively low levels of genera *Lactobacillus* and *Barnesiella* and elevated amounts of *Parasutterella* and *Alistipes* in *App^{NL-G-F}* mice. VSL#3 feeding increased *Clostridia*, *Lachnospiracea* and *Akkermansia* genera in the *App^{NL-G-F}* mice. Gut bacterial metabolites are considered important for neurological function. The chief inhibitory neurotransmitter in the CNS, γ -Aminobutyric acid (GABA), can be produced by *Lactobacillus* and *Bifidobacterium* in the gut. It has been shown that decreased *Lactobacillus* results in a decrease in GABA in the intestines as well as CNS and

correlates with suppression of inflammatory immune response [35]. A recent study suggests an association of *Parasutterella* with increased intestinal inflammation and development of irritable bowel syndrome (IBS) in humans and mice [36]. Additional work supports this indicating that increased abundance of *Parasutterella* is associated with dysbiosis [37]. Therefore, the *Parasutterella* in *App^{NL-G-F}* mice could be contributing to their intestinal dysbiosis and increased inflammation. Increased levels of *Alistipes* and *Enterobacteriaceae* in conjunction with reduced *Faecalibacterium* have been found in patients with depressive disorders [38]. On the other hand, the Akkermansia-induced increase with VSL#3 feeding corresponds well with its role as a probiotic and well characterized immunomodulatory, metabolic, and intestinal protective benefits [39–41].

Alterations in gut microbiota often produce changes in microbial metabolites including SCFAs. Microbiota-derived SCFAs cross the blood brain barrier and play an important role in gut-brain signaling mechanisms. Acetate, propionate, and butyrate are produced in the colon by bacterial fermentation of dietary fibers and are known to have a role in brain function and pathophysiology [42]. For example, changes in plasma as well as fecal SCFA concentrations have been associated with several metabolic disorders [43–45]. We observed a VSL#3-dependent increase in levels of acetate, butyrate, lactate, isobutyrate, and propionate in the serum of *App^{NL-G-F}* mice with only increases in acetate, lactate, and butyrate in WT mice. However, only acetate and lactate were elevated in brains of only *App^{NL-G-F}* mice. The high levels of *Bacteroidetes*, known producers of acetate and propionate, in *App^{NL-G-F}* mice could explain the elevated levels observed in *App^{NL-G-F}* serum [46]. VSL#3 supplementation produced genotype selective effects resulting in decreased *Alistipes*, *Lachnospiraceae*, and *Oscillibacter* in WT mice and an increase in several genera including *Lachnospiraceae*, *Clostridia*, *Akkermansia*, and a decrease as well as decrease in order *Bacteroidales* in *App^{NL-G-F}* mice. *Lactobacillus* are producers of acetate and lactate [47] consistent with the high levels of this genus observed in WT mice and the elevations of these SCFAs in serum of WT animals treated with probiotics. *Akkermansia muciniphila* produce both propionate and acetate suggesting the increased abundance in probiotic fed *App^{NL-G-F}* mice may contribute to the observed elevations in serum and brain [48–50]. A recent human study also showed the effect of altered gut microbiota composition on gut metabolites or tryptophan metabolism in probiotic supplemented AD patients [51]. Although the changes in serum and brain SCFAs were expected based upon prior study of VSL#3 feeding [52], further work is required to determine whether particular SCFAs are responsible for the behavioral or cellular changes we observed in the brain.

For example, butyrate is the main energy source for colonocytes and it is known that most of the butyrate-producing bacteria belong to *Clostridium clusters IV and XIVa*, including *Ruminococcaceae*, *Lachnospiraceae*, and *Butyricoccus* [53]. We observed an increase in serum butyrate in *App^{NL-G-F}* mice fed with VSL#3 corresponding with increased *Lachnospiraceae* and *Clostridium* species. However, no change in butyrate was observed in VSL#3 treated WT mice in agreement with no change in levels of *Lachnospiraceae* and *Clostridia*. Again, this demonstrated a genotype-selective effect of probiotic feeding. Since SCFAs, including butyrate, reportedly increase the growth rate of human neural progenitor cells and increase neurogenesis [54–56], we assessed whether VSL#3 feeding affected neurogenesis in the *App^{NL-G-F}* mice. Indeed, VSL#3 feeding reportedly increases

synaptogenesis and neurogenesis in mice [57, 58] similar to effects seen with intravenous or intraperitoneal administration of sodium butyrate [59, 60]. Although we assessed reduced neurogenesis in *App^{NL-G-F}* mice, we observed no benefit from probiotic feeding. This may be due to the fact that VSL#3 feeding only enhanced serum levels of butyrate with no changes in the brain. Future efforts with prolonged or higher dosage probiotic administration well as improved methods for quantifying neurogenesis are required to fully explore any protective effects on elevating brain butyrate levels and enhancing neurogenesis.

Interestingly, a related branched-chain fatty acid, isobutyrate, solely produced by gut bacteria, was increased in the serum of VSL#3 fed *App^{NL-G-F}* mice. It is unclear why this change was specific to the *App^{NL-G-F}* mice and not also present in the brain. Gut microbes can use the branched-chain amino acids valine, isoleucine, and leucine to generate branched-chain fatty acids such as isobutyrate, 2-methylbutyrate, and isovalerate [61]. A role of isobutyrate on brain function is unknown and determining whether it has a role in the AD-related changes in *App^{NL-G-F}* mice requires further work. However, previous reports suggests that it, along with other SCFAs, could affect the pathophysiology of AD by affecting gliosis, inflammation, and A β /tau aggregation [62].

Although we observed no changes in neurogenesis correlating with brain SCFA levels after probiotic feeding, a recent study showed the capability of SCFAs to potently inhibit A β aggregation *in vitro* [63]. Based upon this we assessed possible effects of probiotic feeding on *App^{NL-G-F}* plaque load. Surprisingly, VSL#3 treatment resulted in no changes in A β levels, plaque load or gliosis. Nevertheless, longer treatment periods or increased dosage of VS#3 in future work may produce effects on A β deposition and subsequent gliotic and inflammatory changes.

In spite of the lack of change in plaques or gliosis, VSL#3 feeding significantly and selectively increased neuronal c-Fos staining only in *App^{NL-G-F}*. c-Fos is a transcription factor widely used as a functional marker of activity in neurons and neuronal circuitry after a variety of stimuli [64]. Increased lactate levels could be involved in modulating the neuronal activity selectively in the *App^{NL-G-F}* mice. Lactate can modulate neuronal excitability via ATP-dependent mechanisms involving modulation of K_{ATP} channels [65]. Lactate has also been shown to induce expression of synaptic plasticity-related genes such as Arc, c-Fos, and Zif268 in neurons through a mechanism involving N-methyl-D-aspartate (NMDA) receptor activity and its downstream signaling cascade mediated by Extracellular signal-regulated kinase (ERK) 1/2 [66]. Alternatively, enhanced neuronal excitability in *App^{NL-G-F}* mice treated with VSL#3 might be due to altered neurotransmitter levels in the brain following probiotic treatment. Gut bacteria produce and/or consume a wide range of neurotransmitters, including dopamine, norepinephrine, serotonin, and GABA [67]. c-Fos and other immediate early genes are known to be highly responsive to extracellular stimulation by neurotransmitters, membrane depolarization, and trophic substances [68, 69]. The mechanism or consequences of elevated c-Fos expression and presumed neuronal activity in VSL#3 fed *App^{NL-G-F}* mice likely involve complex changes such as epigenetic modifications and will require additional effort to define [70].

In summary, our study demonstrates that the probiotic, VSL#3, affects control and diseased mice by uniquely induced differences in gut bacterial composition and SCFA concentration changes in both serum and brain. *App^{NL-G-F}* mice had a disease- but not treatment-specific elevation of brain isobutyrate levels. Although probiotic treatment did not alter plaque load or gliosis, it did increase brain lactate levels in *App^{NL-G-F}* mice correlating with increased c-Fos inferred neuronal activity and reduced anxiety-like behavior. Further effort with increased dose/duration or younger age of treatment onset using probiotics such as VSL#3 may provide robust effects on brain presentation of AD.

Acknowledgement

This work was supported by funding from Alzheimer's Association Research fellowship, AARF-17-533143, a University of North Dakota (UND) Post-Doc Pilot Grant, the North Dakota Experimental Program to Stimulate Competitive Research (ND EPSCoR), UND0021228, and National Institutes of Health (NIH) 5R01AG048993, 5P20GM113123, and P20GM103442 and U54GM128729. D. Darland is supported by NIH/Center for Biomedical Research Excellence 2P20GM104360-06A1 (R. Vaughan, PI; D. Darland Project Leader). We thank Drs. Takashi Saito and Takaomi Saido, Laboratory for Proteolytic Neuroscience, RIKEN Center for Brain Science, Wako, Saitama, Japan for kindly providing *App^{NL-G-F}* mice. The authors also thank Angela M. Floden, Dr. Gunjan D. Manocha, Dr. Joshua A. Kulas, and Mona Sohrabi for their help in animal/tissue collection.

References

- [1]. Kametani F, Hasegawa M (2018) Reconsideration of Amyloid Hypothesis and Tau Hypothesis in Alzheimer's Disease. *Front Neurosci* 12, 25. [PubMed: 29440986]
- [2]. Coon KD, Myers AJ, Craig DW, Webster JA, Pearson JV, Lince DH, Zismann VL, Beach TG, Leung D, Bryden L, Halperin RF, Marlowe L, Kaleem M, Walker DG, Ravid R, Heward CB, Rogers J, Papassotiropoulos A, Reiman EM, Hardy J, Stephan DA (2007) A high-density whole-genome association study reveals that APOE is the major susceptibility gene for sporadic late-onset Alzheimer's disease. *J Clin Psychiatry* 68, 613–618. [PubMed: 17474819]
- [3]. Calderon-Garciduenas L, Reed W, Maronpot RR, Henriquez-Roldan C, Delgado-Chavez R, Calderon-Garciduenas A, Dragustinovis I, Franco-Lira M, Aragon-Flores M, Solt AC, Altenburg M, Torres-Jardon R, Swenberg JA (2004) Brain inflammation and Alzheimer's-like pathology in individuals exposed to severe air pollution. *Toxicol Pathol* 32, 650–658. [PubMed: 15513908]
- [4]. Yegambaram M, Manivannan B, Beach TG, Halden RU (2015) Role of environmental contaminants in the etiology of Alzheimer's disease: a review. *Curr Alzheimer Res* 12, 116–146. [PubMed: 25654508]
- [5]. Pistollato F, Sumalla Cano S, Elio I, Masias Vergara M, Giampieri F, Battino M (2016) Role of gut microbiota and nutrients in amyloid formation and pathogenesis of Alzheimer disease. *Nutr Rev* 74, 624–634. [PubMed: 27634977]
- [6]. Itzhaki RF, Lathe R, Balin BJ, Ball MJ, Bearer EL, Braak H, Bullido MJ, Carter C, Clerici M, Cosby SL, Del Tredici K, Field H, Fulop T, Grassi C, Griffin WS, Haas J, Hudson AP, Kamer AR, Kell DB, Licastro F, Letenneur L, Lovheim H, Mancuso R, Miklossy J, Otth C, Palamara AT, Perry G, Preston C, Pretorius E, Strandberg T, Tabet N, Taylor-Robinson SD, Whittum-Hudson JA (2016) Microbes and Alzheimer's Disease. *J Alzheimers Dis* 51, 979–984. [PubMed: 26967229]
- [7]. Vogt NM, Kerby RL, Dill-McFarland KA, Harding SJ, Merluzzi AP, Johnson SC, Carlsson CM, Asthana S, Zetterberg H, Blennow K, Bendlin BB, Rey FE (2017) Gut microbiome alterations in Alzheimer's disease. *Sci Rep* 7, 13537. [PubMed: 29051531]
- [8]. MahmoudianDehkordi S, Arnold M, Nho K, Ahmad S, Jia W, Xie G, Louie G, Kueider-Paisley A, Moseley MA, Thompson JW, St John Williams L, Tenenbaum JD, Blach C, Baillie R, Han X, Bhattacharyya S, Toledo JB, Schafferer S, Klein S, Koal T, Risacher SL, Kling MA, Motsinger-Reif A, Rotroff DM, Jack J, Hankemeier T, Bennett DA, De Jager PL, Trojanowski JQ, Shaw LM, Weiner MW, Doraiswamy PM, van Duijn CM, Saykin AJ, Kastenmuller G, Kaddurah-Daouk R, Alzheimer's Disease Neuroimaging I, the Alzheimer Disease Metabolomics C (2019)

- Altered bile acid profile associates with cognitive impairment in Alzheimer's disease-An emerging role for gut microbiome. *Alzheimers Dement* 15, 76–92. [PubMed: 30337151]
- [9]. Vogt NM, Romano KA, Darst BF, Engelman CD, Johnson SC, Carlsson CM, Asthana S, Blennow K, Zetterberg H, Bendlin BB, Rey FE (2018) The gut microbiota-derived metabolite trimethylamine N-oxide is elevated in Alzheimer's disease. *Alzheimers Res Ther* 10, 124. [PubMed: 30579367]
- [10]. Bengmark S (2013) Gut microbiota, immune development and function. *Pharmacol Res* 69, 87–113. [PubMed: 22989504]
- [11]. Collins SM, Surette M, Bercik P (2012) The interplay between the intestinal microbiota and the brain. *Nat Rev Microbiol* 10, 735–742. [PubMed: 23000955]
- [12]. Diamond B, Huerta PT, Tracey K, Volpe BT (2011) It takes guts to grow a brain: Increasing evidence of the important role of the intestinal microflora in neuro- and immune-modulatory functions during development and adulthood. *Bioessays* 33, 588–591. [PubMed: 21681774]
- [13]. Rogers GB, Keating DJ, Young RL, Wong ML, Licinio J, Wesselingh S (2016) From gut dysbiosis to altered brain function and mental illness: mechanisms and pathways. *Mol Psychiatry* 21, 738–748. [PubMed: 27090305]
- [14]. Giau VV, Wu SY, Jamerlan A, An SSA, Kim SY, Hulme J (2018) Gut Microbiota and Their Neuroinflammatory Implications in Alzheimer's Disease. *Nutrients* 10.
- [15]. Org E, Blum Y, Kasela S, Mehrabian M, Kuusisto J, Kangas AJ, Soininen P, Wang Z, Ala-Korpela M, Hazen SL, Laakso M, Lusa AJ (2017) Relationships between gut microbiota, plasma metabolites, and metabolic syndrome traits in the METSIM cohort. *Genome Biol* 18, 70. [PubMed: 28407784]
- [16]. Arora T, Backhed F (2016) The gut microbiota and metabolic disease: current understanding and future perspectives. *J Intern Med* 280, 339–349. [PubMed: 27071815]
- [17]. Canfora EE, Meex RCR, Venema K, Blaak EE (2019) Gut microbial metabolites in obesity, NAFLD and T2DM. *Nat Rev Endocrinol* 15, 261–273. [PubMed: 30670819]
- [18]. Qin J, Li R, Raes J, Arumugam M, Burgdorf KS, Manichanh C, Nielsen T, Pons N, Levenez F, Yamada T, Mende DR, Li J, Xu J, Li S, Li D, Cao J, Wang B, Liang H, Zheng H, Xie Y, Tap J, Lepage P, Bertalan M, Batto JM, Hansen T, Le Paslier D, Linneberg A, Nielsen HB, Pelletier E, Renault P, Sicheritz-Ponten T, Turner K, Zhu H, Yu C, Li S, Jian M, Zhou Y, Li Y, Zhang X, Li S, Qin N, Yang H, Wang J, Brunak S, Dore J, Guarner F, Kristiansen K, Pedersen O, Parkhill J, Weissenbach J, Meta HITC, Bork P, Ehrlich SD, Wang J (2010) A human gut microbial gene catalogue established by metagenomic sequencing. *Nature* 464, 59–65. [PubMed: 20203603]
- [19]. Cummings JH, Pomare EW, Branch WJ, Naylor CP, Macfarlane GT (1987) Short chain fatty acids in human large intestine, portal, hepatic and venous blood. *Gut* 28, 1221–1227. [PubMed: 3678950]
- [20]. Macfarlane GT, Macfarlane S (2012) Bacteria, colonic fermentation, and gastrointestinal health. *J AOAC Int* 95, 50–60. [PubMed: 22468341]
- [21]. Zoetendal EG, de Vos WM (2014) Effect of diet on the intestinal microbiota and its activity. *Curr Opin Gastroenterol* 30, 189–195. [PubMed: 24457346]
- [22]. Saito T, Matsuba Y, Mihira N, Takano J, Nilsson P, Itohara S, Iwata N, Saido TC (2014) Single App knock-in mouse models of Alzheimer's disease. *Nat Neurosci* 17, 661–663. [PubMed: 24728269]
- [23]. Reagan-Shaw S, Nihal M, Ahmad N (2008) Dose translation from animal to human studies revisited. *FASEB J* 22, 659–661. [PubMed: 17942826]
- [24]. Tursi A, Brandimarte G, Papa A, Giglio A, Elisei W, Giorgetti GM, Forti G, Morini S, Hassan C, Pistoia MA, Modeo ME, Rodino S, D'Amico T, Sebkova L, Sacca N, Di Giulio E, Lizza F, Imeneo M, Larussa T, Di Rosa S, Annese V, Danese S, Gasbarrini A (2010) Treatment of relapsing mild-to-moderate ulcerative colitis with the probiotic VSL#3 as adjunctive to a standard pharmaceutical treatment: a double-blind, randomized, placebo-controlled study. *Am J Gastroenterol* 105, 2218–2227. [PubMed: 20517305]
- [25]. Dhiman RK, Rana B, Agrawal S, Garg A, Chopra M, Thumburu KK, Khattri A, Malhotra S, Duseja A, Chawla YK (2014) Probiotic VSL#3 reduces liver disease severity and hospitalization

- in patients with cirrhosis: a randomized, controlled trial. *Gastroenterology* 147, 1327–1337 e1323. [PubMed: 25450083]
- [26]. Torii T, Kanemitsu K, Wada T, Itoh S, Kinugawa K, Hagiwara A (2010) Measurement of short-chain fatty acids in human faeces using high-performance liquid chromatography: specimen stability. *Ann Clin Biochem* 47, 447–452. [PubMed: 20595408]
- [27]. Brose SA, Baker AG, Golovko MY (2013) A fast one-step extraction and UPLC-MS/MS analysis for E2/D 2 series prostaglandins and isoprostanes. *Lipids* 48, 411–419. [PubMed: 23400687]
- [28]. Brose SA, Marquardt AL, Golovko MY (2014) Fatty acid biosynthesis from glutamate and glutamine is specifically induced in neuronal cells under hypoxia. *J Neurochem* 129, 400–412. [PubMed: 24266789]
- [29]. Nagamoto-Combs K, Manocha GD, Puig K, Combs CK (2016) An improved approach to align and embed multiple brain samples in a gelatin-based matrix for simultaneous histological processing. *J Neurosci Methods* 261, 155–160. [PubMed: 26743972]
- [30]. Dhawan G, Combs CK (2012) Inhibition of Src kinase activity attenuates amyloid associated microgliosis in a murine model of Alzheimer's disease. *J Neuroinflammation* 9, 117. [PubMed: 22673542]
- [31]. Manocha GD, Floden AM, Rausch K, Kulas JA, McGregor BA, Rojanathammanee L, Puig KR, Puig KL, Karki S, Nichols MR, Darland DC, Porter JE, Combs CK (2016) APP Regulates Microglial Phenotype in a Mouse Model of Alzheimer's Disease. *J Neurosci* 36, 8471–8486. [PubMed: 27511018]
- [32]. Pardo M, Betz AJ, San Miguel N, Lopez-Cruz L, Salamone JD, Correa M (2013) Acetate as an active metabolite of ethanol: studies of locomotion, loss of righting reflex, and anxiety in rodents. *Front Behav Neurosci* 7, 81. [PubMed: 23847487]
- [33]. Ogbonnaya ES, Clarke G, Shanahan F, Dinan TG, Cryan JF, O'Leary OF (2015) Adult Hippocampal Neurogenesis Is Regulated by the Microbiome. *Biol Psychiatry* 78, e7–9. [PubMed: 25700599]
- [34]. Santos PL, Brito RG, Matos J, Quintans JSS, Quintans-Junior LJ (2018) Fos Protein as a Marker of Neuronal Activity: a Useful Tool in the Study of the Mechanism of Action of Natural Products with Analgesic Activity. *Mol Neurobiol* 55, 4560–4579. [PubMed: 28695537]
- [35]. Szablewski L (2018) Human Gut Microbiota in Health and Alzheimer's Disease. *J Alzheimers Dis* 62, 549–560. [PubMed: 29480188]
- [36]. Chen YJ, Wu H, Wu SD, Lu N, Wang YT, Liu HN, Dong L, Liu TT, Shen XZ (2018) Parasutterella, in association with irritable bowel syndrome and intestinal chronic inflammation. *J Gastroenterol Hepatol* 33, 1844–1852. [PubMed: 29744928]
- [37]. Chiodini RJ, Dowd SE, Chamberlin WM, Galandiuk S, Davis B, Glassing A (2015) Microbial Population Differentials between Mucosal and Submucosal Intestinal Tissues in Advanced Crohn's Disease of the Ileum. *PLoS One* 10, e0134382. [PubMed: 26222621]
- [38]. Huang TT, Lai JB, Du YL, Xu Y, Ruan LM, Hu SH (2019) Current Understanding of Gut Microbiota in Mood Disorders: An Update of Human Studies. *Front Genet* 10, 98. [PubMed: 30838027]
- [39]. Bian X, Wu W, Yang L, Lv L, Wang Q, Li Y, Ye J, Fang D, Wu J, Jiang X, Shi D, Li L (2019) Administration of Akkermansia muciniphila Ameliorates Dextran Sulfate Sodium-Induced Ulcerative Colitis in Mice. *Front Microbiol* 10, 2259. [PubMed: 31632373]
- [40]. Ashrafian F, Shahriary A, Behrouzi A, Moradi HR, Keshavarz Azizi Raftar S, Lari A, Hadifar S, Yaghoobfar R, Ahmadi Badi S, Khatami S, Vaziri F, Siadat SD (2019) Akkermansia muciniphila-Derived Extracellular Vesicles as a Mucosal Delivery Vector for Amelioration of Obesity in Mice. *Front Microbiol* 10, 2155. [PubMed: 31632356]
- [41]. Zhai R, Xue X, Zhang L, Yang X, Zhao L, Zhang C (2019) Strain-Specific Anti-inflammatory Properties of Two Akkermansia muciniphila Strains on Chronic Colitis in Mice. *Front Cell Infect Microbiol* 9, 239. [PubMed: 31334133]
- [42]. Pascale A, Marchesi N, Marelli C, Coppola A, Luzi L, Govoni S, Giustina A, Gazzaruso C (2018) Microbiota and metabolic diseases. *Endocrine* 61, 357–371. [PubMed: 29721802]
- [43]. Sanna S, van Zuydam NR, Mahajan A, Kurilshikov A, Vich Vila A, Vosa U, Mujagic Z, Masclee AAM, Jonkers D, Oosting M, Joosten LAB, Netea MG, Franke L, Zhernakova A, Fu J,

- Wijmenga C, McCarthy MI (2019) Causal relationships among the gut microbiome, short-chain fatty acids and metabolic diseases. *Nat Genet* 51, 600–605. [PubMed: 30778224]
- [44]. Chambers ES, Preston T, Frost G, Morrison DJ (2018) Role of Gut Microbiota-Generated Short-Chain Fatty Acids in Metabolic and Cardiovascular Health. *Curr Nutr Rep* 7, 198–206. [PubMed: 30264354]
- [45]. de la Cuesta-Zuluaga J, Mueller NT, Alvarez-Quintero R, Velasquez-Mejia EP, Sierra JA, Corrales-Agudelo V, Carmona JA, Abad JM, Escobar JS (2018) Higher Fecal Short-Chain Fatty Acid Levels Are Associated with Gut Microbiome Dysbiosis, Obesity, Hypertension and Cardiometabolic Disease Risk Factors. *Nutrients* 11.
- [46]. Levy M, Thaiss CA, Elinav E (2016) Metabolites: messengers between the microbiota and the immune system. *Genes Dev* 30, 1589–1597. [PubMed: 27474437]
- [47]. Slavica A, Trontel A, Jelovac N, Kosovec Z, Santek B, Novak S (2015) Production of lactate and acetate by *Lactobacillus coryniformis* subsp. *torquens* DSM 20004(T) in comparison with *Lactobacillus amylovorus* DSM 20531(T). *J Biotechnol* 202, 50–59. [PubMed: 25617683]
- [48]. Louis P, Flint HJ (2017) Formation of propionate and butyrate by the human colonic microbiota. *Environ Microbiol* 19, 29–41. [PubMed: 27928878]
- [49]. Derrien M, Vaughan EE, Plugge CM, de Vos WM (2004) *Akkermansia muciniphila* gen. nov., sp. nov., a human intestinal mucin-degrading bacterium. *Int J Syst Evol Microbiol* 54, 1469–1476. [PubMed: 15388697]
- [50]. Parada Venegas D, De la Fuente MK, Landskron G, Gonzalez MJ, Quera R, Dijkstra G, Harmsen HJM, Faber KN, Hermoso MA (2019) Short Chain Fatty Acids (SCFAs)-Mediated Gut Epithelial and Immune Regulation and Its Relevance for Inflammatory Bowel Diseases. *Front Immunol* 10, 277. [PubMed: 30915065]
- [51]. Leblhuber F, Steiner K, Schuetz B, Fuchs D, Gostner JM (2018) Probiotic Supplementation in Patients with Alzheimer's Dementia - An Explorative Intervention Study. *Curr Alzheimer Res* 15, 1106–1113. [PubMed: 30101706]
- [52]. Yadav H, Lee JH, Lloyd J, Walter P, Rane SG (2013) Beneficial metabolic effects of a probiotic via butyrate-induced GLP-1 hormone secretion. *J Biol Chem* 288, 25088–25097. [PubMed: 23836895]
- [53]. Topping DL, Clifton PM (2001) Short-chain fatty acids and human colonic function: roles of resistant starch and nonstarch polysaccharides. *Physiol Rev* 81, 1031–1064. [PubMed: 11427691]
- [54]. Kim HJ, Leeds P, Chuang DM (2009) The HDAC inhibitor, sodium butyrate, stimulates neurogenesis in the ischemic brain. *J Neurochem* 110, 1226–1240. [PubMed: 19549282]
- [55]. Yoo DY, Kim W, Nam SM, Kim DW, Chung JY, Choi SY, Yoon YS, Won MH, Hwang IK (2011) Synergistic effects of sodium butyrate, a histone deacetylase inhibitor, on increase of neurogenesis induced by pyridoxine and increase of neural proliferation in the mouse dentate gyrus. *Neurochem Res* 36, 1850–1857. [PubMed: 21597935]
- [56]. Yang LL, Millischer V, Rodin S, MacFabe DF, Villaescusa JC, Lavebratt C (2019) Enteric short-chain fatty acids promote proliferation of human neural progenitor cells. *J Neurochem*, e14928.
- [57]. Mohle L, Mattei D, Heimesaat MM, Bereswill S, Fischer A, Alutis M, French T, Hambardzumyan D, Matzinger P, Dunay IR, Wolf SA (2016) Ly6C(hi) Monocytes Provide a Link between Antibiotic-Induced Changes in Gut Microbiota and Adult Hippocampal Neurogenesis. *Cell Rep* 15, 1945–1956. [PubMed: 27210745]
- [58]. Distrutti E, O'Reilly JA, McDonald C, Cipriani S, Renga B, Lynch MA, Fiorucci S (2014) Modulation of intestinal microbiota by the probiotic VSL#3 resets brain gene expression and ameliorates the age-related deficit in LTP. *PLoS One* 9, e106503. [PubMed: 25202975]
- [59]. Braniste V, Al-Asmakh M, Kowal C, Anuar F, Abbaspour A, Toth M, Korecka A, Bakocevic N, Ng LG, Kundu P, Gulyas B, Halldin C, Hultenby K, Nilsson H, Hebert H, Volpe BT, Diamond B, Pettersson S (2014) The gut microbiota influences blood-brain barrier permeability in mice. *Sci Transl Med* 6, 263ra158.
- [60]. Li H, Sun J, Wang F, Ding G, Chen W, Fang R, Yao Y, Pang M, Lu ZQ, Liu J (2016) Sodium butyrate exerts neuroprotective effects by restoring the blood-brain barrier in traumatic brain injury mice. *Brain Res* 1642, 70–78. [PubMed: 27017959]

- [61]. Smith EA, Macfarlane GT (1997) Dissimilatory amino Acid metabolism in human colonic bacteria. *Anaerobe* 3, 327–337. [PubMed: 16887608]
- [62]. Bostanciklioglu M (2019) The role of gut microbiota in pathogenesis of Alzheimer’s disease. *J Appl Microbiol* 127, 954–967. [PubMed: 30920075]
- [63]. Ho L, Ono K, Tsuji M, Mazzola P, Singh R, Pasinetti GM (2018) Protective roles of intestinal microbiota derived short chain fatty acids in Alzheimer’s disease-type beta-amyloid neuropathological mechanisms. *Expert Rev Neurother* 18, 83–90. [PubMed: 29095058]
- [64]. Kovacs KJ (1998) c-Fos as a transcription factor: a stressful (re)view from a functional map. *Neurochem Int* 33, 287–297. [PubMed: 9840219]
- [65]. Belanger M, Allaman I, Magistretti PJ (2011) Brain energy metabolism: focus on astrocyte-neuron metabolic cooperation. *Cell Metab* 14, 724–738. [PubMed: 22152301]
- [66]. Yang J, Ruchti E, Petit JM, Jourdain P, Grenningloh G, Allaman I, Magistretti PJ (2014) Lactate promotes plasticity gene expression by potentiating NMDA signaling in neurons. *Proc Natl Acad Sci U S A* 111, 12228–12233. [PubMed: 25071212]
- [67]. Strandwitz P (2018) Neurotransmitter modulation by the gut microbiota. *Brain Res* 1693, 128–133. [PubMed: 29903615]
- [68]. Chaudhuri A, Zangenehpour S, Rahbar-Dehgan F, Ye F (2000) Molecular maps of neural activity and quiescence. *Acta Neurobiol Exp (Wars)* 60, 403–410. [PubMed: 11016083]
- [69]. Kawasaki M, Ponzio TA, Yue C, Fields RL, Gainer H (2009) Neurotransmitter regulation of c-fos and vasopressin gene expression in the rat supraoptic nucleus. *Exp Neurol* 219, 212–222. [PubMed: 19463813]
- [70]. Lahiri DK, Maloney B (2010) The “LEARn” (Latent Early-life Associated Regulation) model integrates environmental risk factors and the developmental basis of Alzheimer’s disease, and proposes remedial steps. *Exp Gerontol* 45, 291–296. [PubMed: 20064601]

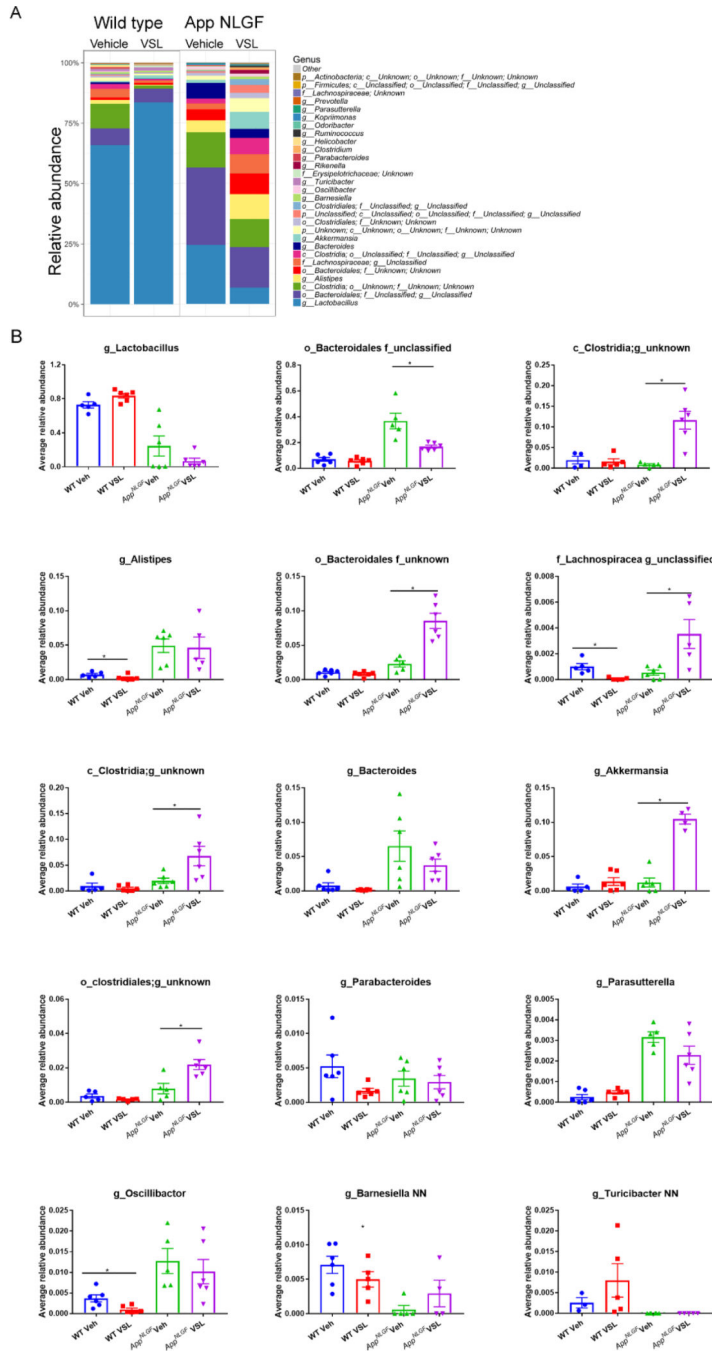
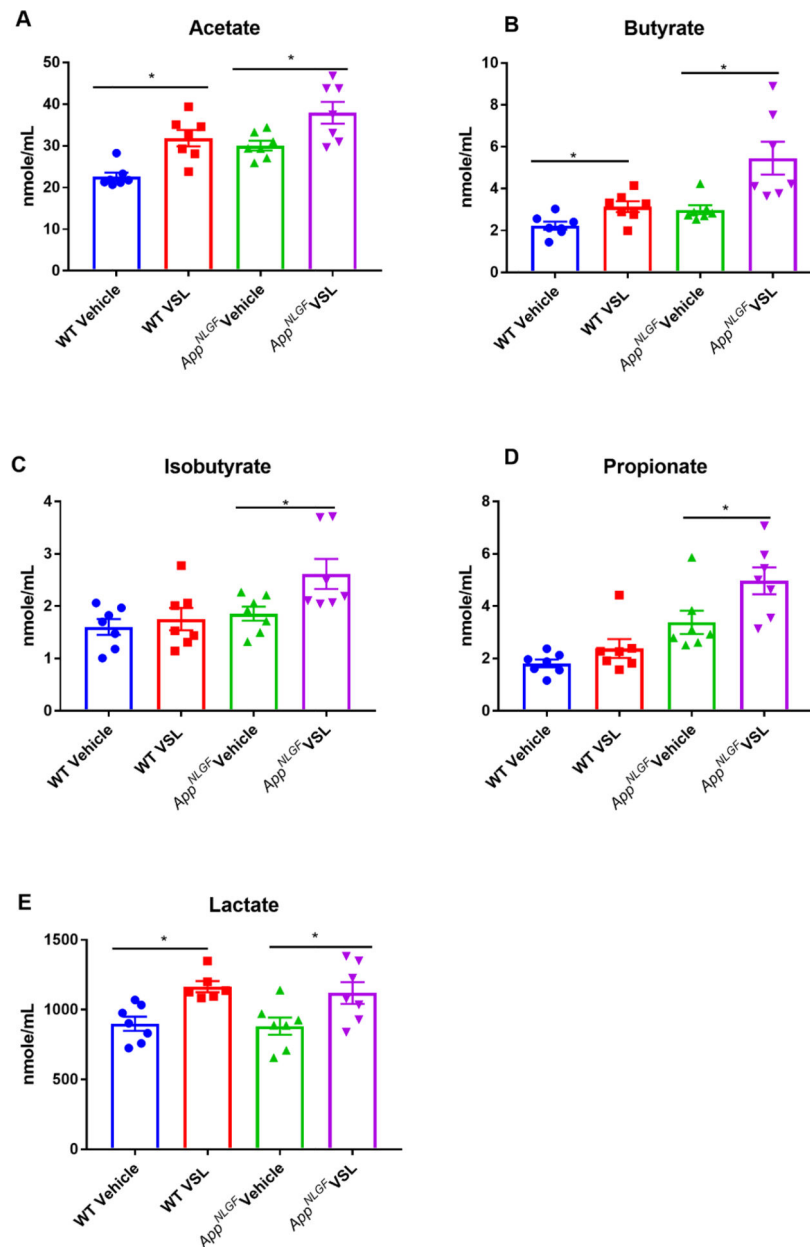


Fig. 1. Effects of VSL#3 probiotic supplementation on fecal bacterial genus profile in *App^{NL-G-F}* and wild type mice. Fecal samples were collected from female C57BL/6 wild type and *App^{NL-G-F}* mice with and without *ad libitum* VSL#3 in the drinking water from 6–8 months of age. Bacterial genera were determined from 16S rRNA sequencing. (A). Relative abundances of the 30 most abundant fecal genera in stool samples of wild type (WT) and *App^{NL-G-F}* mice are graphed. (B). The relative abundances of the top 15 most abundant genera across the treatment groups were statistically compared. Operational taxonomic units

(OTUs) of some samples lacked a taxonomy label at the genus level and are represented as order or family only. 6 animals per group were examined. Data are presented as mean values \pm standard error of mean (SEM). Significant differences between vehicle and VSL#3 treated animals in each genotype were determined by Mann–Whitney test, * $p < 0.05$.



29

Fig. 2. Effects of VSL#3 supplementation on serum concentrations of short chain fatty acids (SCFAs) (A) acetate, (B) butyrate, (C) isobutyrate, (D) lactate and (E) propionate. Female C57BL/6 wild type and *App^{NL-G-F}* mice were provided normal drinking water or water supplemented with probiotic, VSL#3, *ad libitum* from 6–8 months of age. Blood was collected upon termination and centrifuged to collect serum for SCFA analysis performed using UPLC-MS/MS. Seven animals per group were examined. Data are presented as mean

± SEM. Significant differences between vehicle and VSL#3 treated animals in each genotype were determined by t-test; *p<0.05.

Author Manuscript

Author Manuscript

Author Manuscript

Author Manuscript

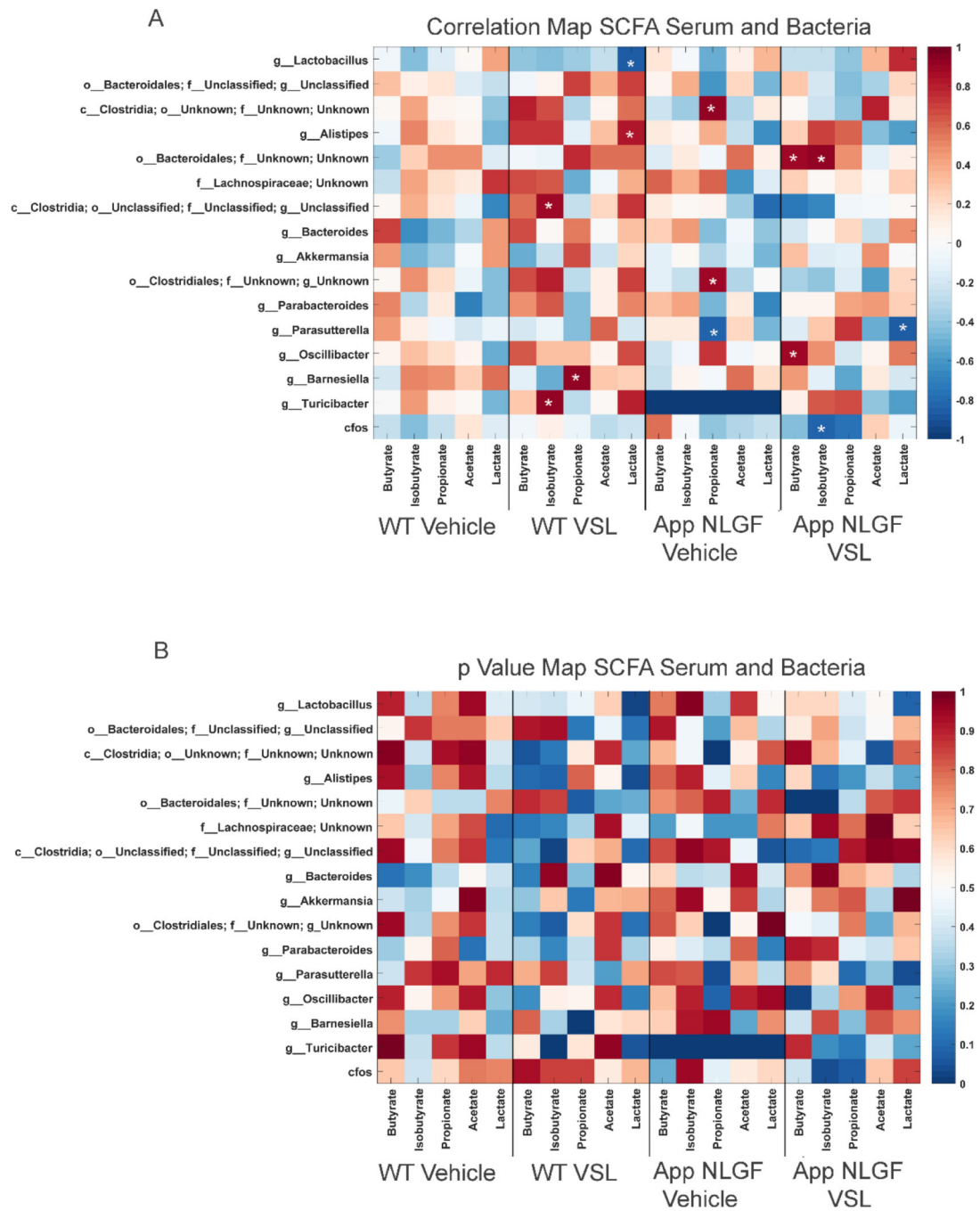


Fig. 3. Comparison of serum SCFAs and fecal microbiome bacteria in C57BL/6 (WT) and *App^{NL-G-F}* mice. Heat maps are presented of the Pearson correlation (A) and the p value (B) of serum SCFAs and fecal bacterial composition. Asterisks in (A) indicate statistically significant positive or negative correlation.

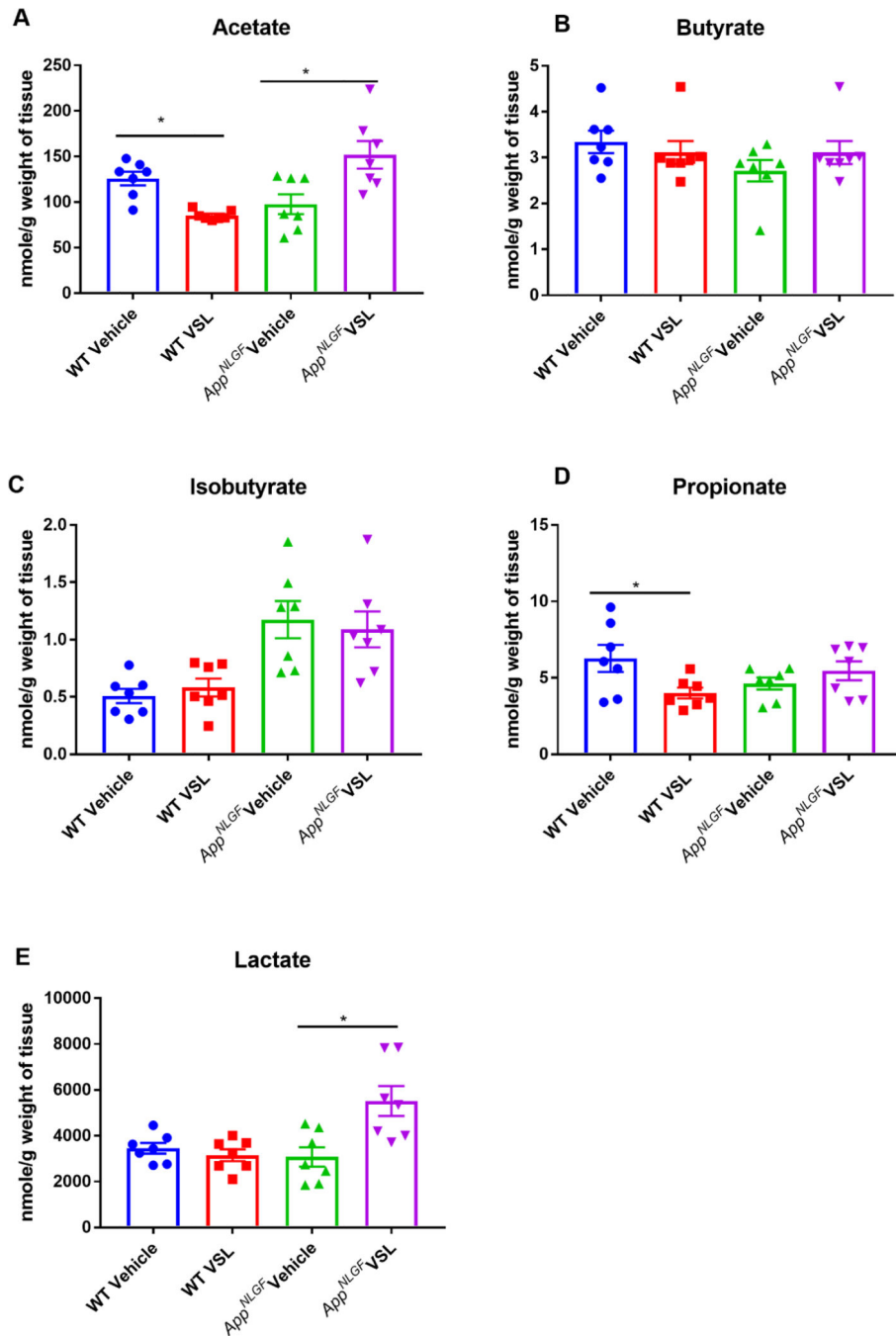


Fig. 4. Effect of VSL#3 supplementation on hippocampal concentrations of short chain fatty acids (SCFA) (A) acetate, (B) butyrate, (C) isobutyrate, (D) lactate and (E) propionate. Female C57BL/6 wild type and *App^{NL-G-F}* mice were provided normal drinking water or water supplemented with probiotic, VSL#3, *ad libitum* for four weeks from 6–8 months of age. Hippocampi were isolated, and concentrations of SCFA, were analyzed using UPLC-MS/MS. Seven animals per group were examined. Data are presented as mean \pm SEM.

Significant differences between vehicle and VSL#3 treated animals in each genotype were determined by t-test; * $p < 0.05$.

Author Manuscript

Author Manuscript

Author Manuscript

Author Manuscript

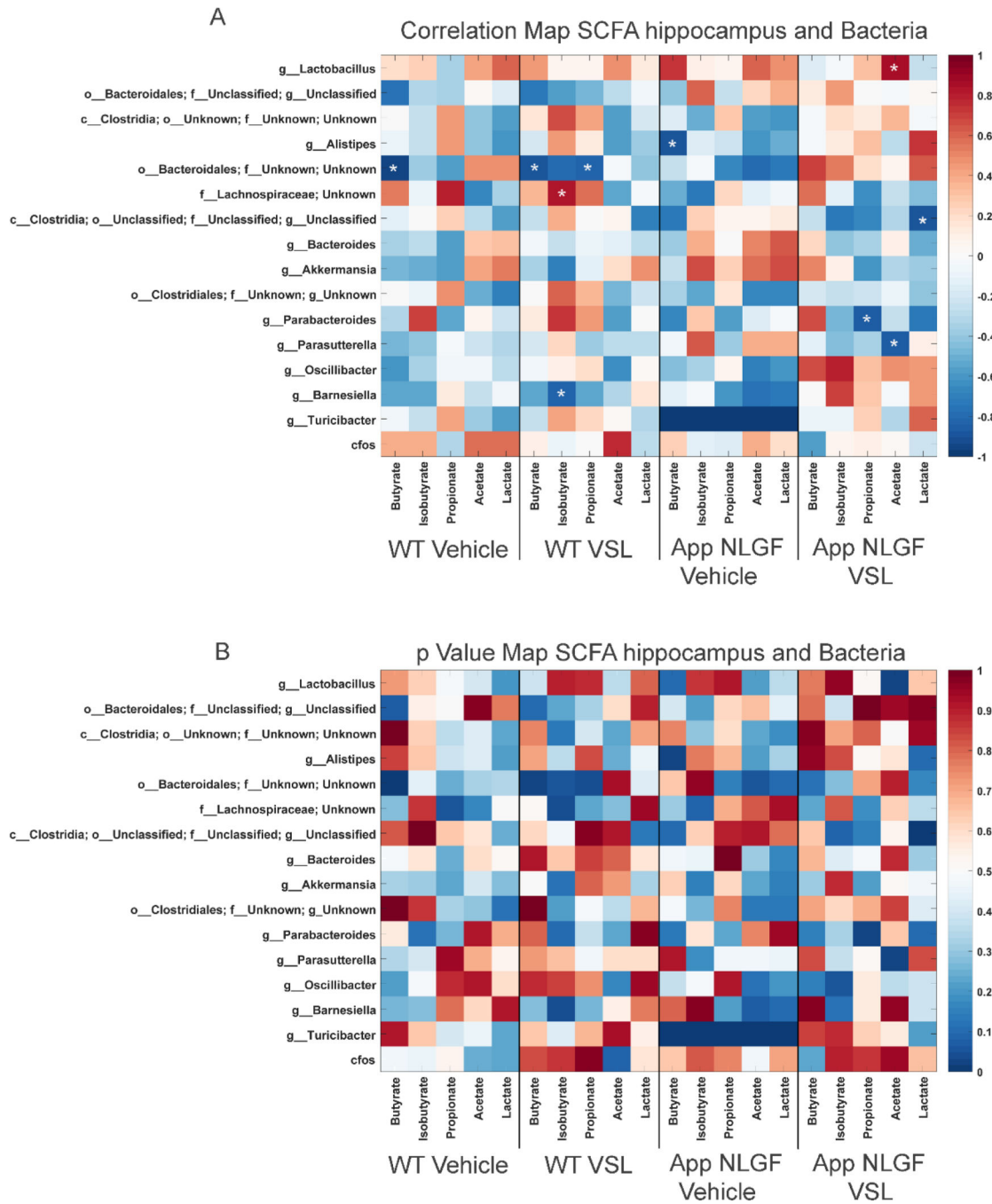


Fig. 5. Comparison of hippocampal SCFAs and fecal microbiome bacteria in C57BL/6 (WT) and *App^{NL-G-F}* mice. Heat maps are presented of the Pearson correlation of (A) and the p value for hippocampal SCFAs and fecal bacterial composition. Asterisks in (A) indicate statistically significant positive or negative correlation.

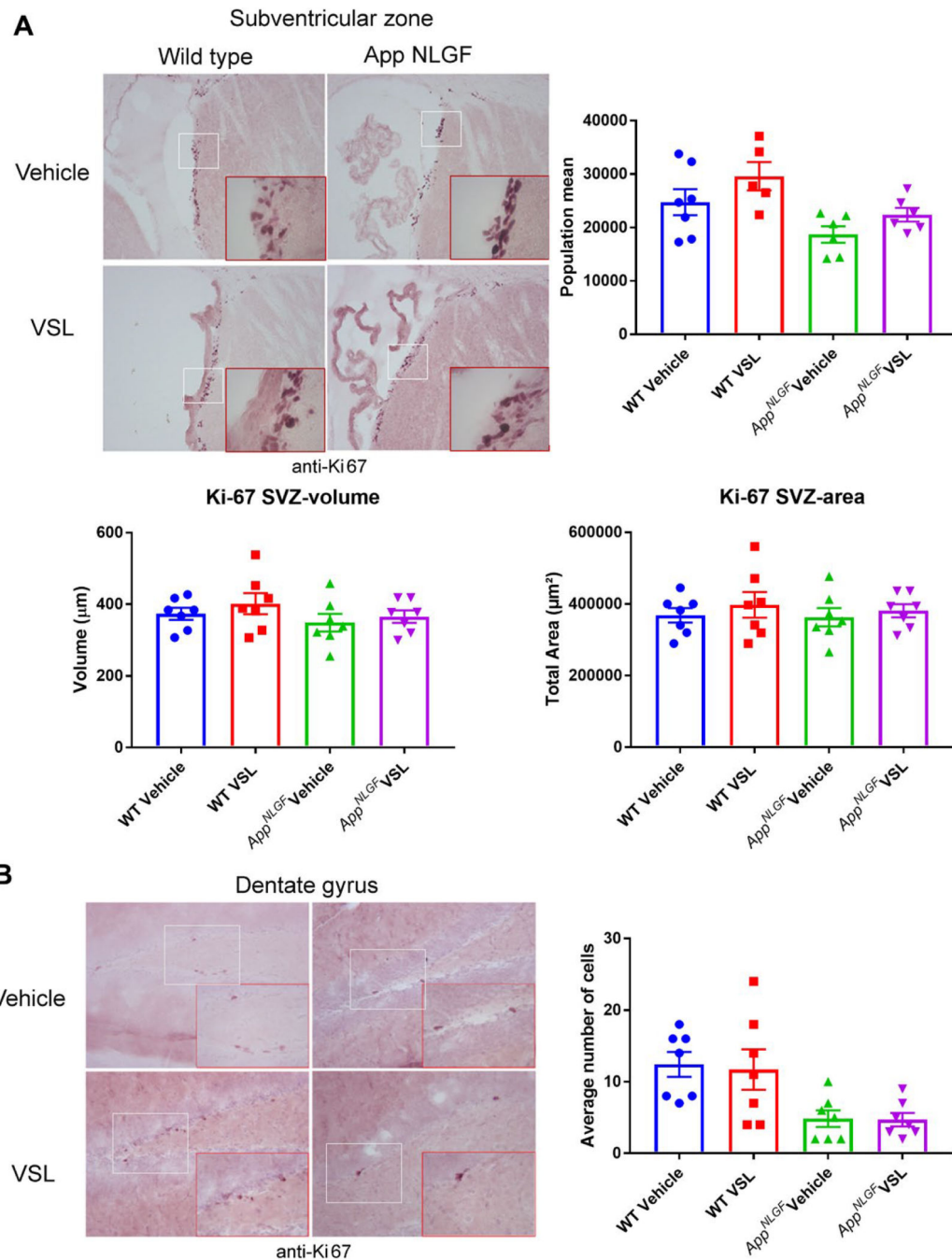


Fig. 6. Effect of VSL#3 supplementation on neurogenesis in the subventricular zone (SVZ) and dentate gyrus of the hippocampus. Brain sections from female C57BL/6 wild type and *App^{NL-G-F}* mice with and without VSL#3 supplementation from 6–8 months were stained with Ki-67 antibody. Seven animals per group were examined and Ki-67 positive cells were counted in 4 sections from each animal. Stereological quantification was done in the (A) SVZ region to count Ki-67 positive cells. (B) However, manual counting was done in the DG due to the limited numbers of detectable Ki-67 positive cells. Representative images are

shown, and data are presented as mean \pm SEM. Significant differences between vehicle and VSL#3 treated animals in each genotype were determined by t-test; * $p < 0.05$.

Author Manuscript

Author Manuscript

Author Manuscript

Author Manuscript

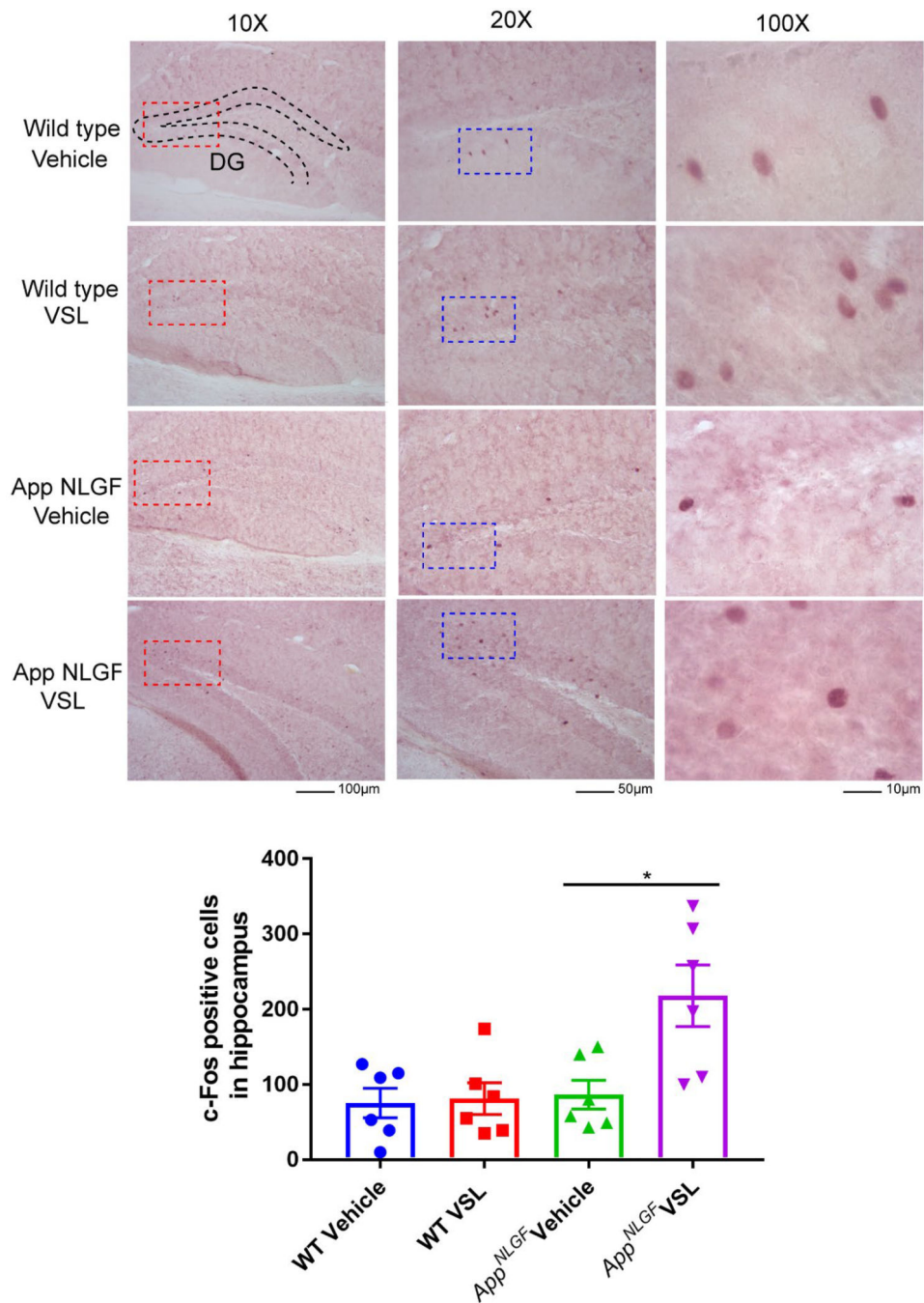


Fig. 7. Effect of VSL#3 dietary supplementation on hippocampal c-Fos immunoreactivity. Female C57BL/6 wild type and *App^{NL-G-F}* mice were provided normal drinking water or water supplemented with probiotic, VSL#3, *ad libitum* from 6–8 months of age. Brain sections from each treatment group were stained with anti-c-Fos antibody (purple labeling). Representative images of dentate gyrus (DG) of hippocampi are shown at 10X, 20X and 100X magnification with the positive cells clearly visible at the higher magnifications and the anatomical references points indicated for dentate gyrus. The positive cells were counted

and values were averaged from 3 sections per brain. Six animals per group were examined and the data are presented as the mean \pm SEM. Significant differences between vehicle and VSL#3 treated animals in each genotype were determined by t-test; * $p < 0.05$.

Author Manuscript

Author Manuscript

Author Manuscript

Author Manuscript

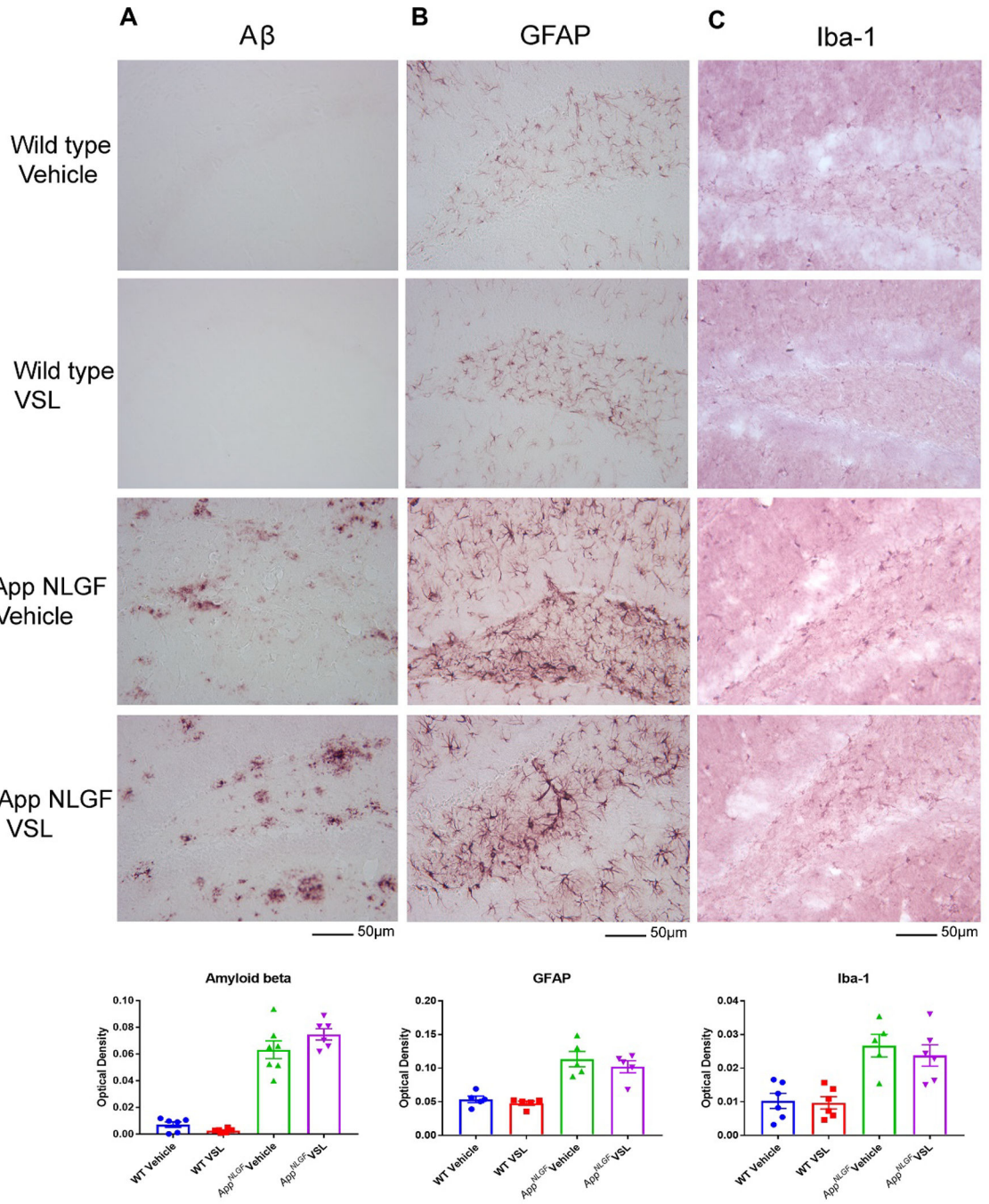


Fig 8. Effect of VSL#3 supplementation on $A\beta$ accumulation and gliosis in brains of C57BL/6 (WT) and App^{NL-G-F} mice. Female C57BL/6 wild type and App^{NL-G-F} mice were provided normal drinking water or water supplemented with probiotic, VSL#3, *ad libitum* from 6–8 months of age. Brain sections were immunolabeled for (A) $A\beta$, (B) GFAP, and (C) Iba-1. Representative images from the hippocampus are shown from the hippocampus region and were taken at 20X. Quantitation of immunolabeling was performed using optical density values and the data are presented as mean \pm SEM. Significant differences between vehicle

Author Manuscript

Author Manuscript

Author Manuscript

Author Manuscript

and VSL#3 treated animals in each genotype were determined by t-test; * $p < 0.05$ (n=7).
Scale bar is 50 μ m.

Author Manuscript

Author Manuscript

Author Manuscript

Author Manuscript

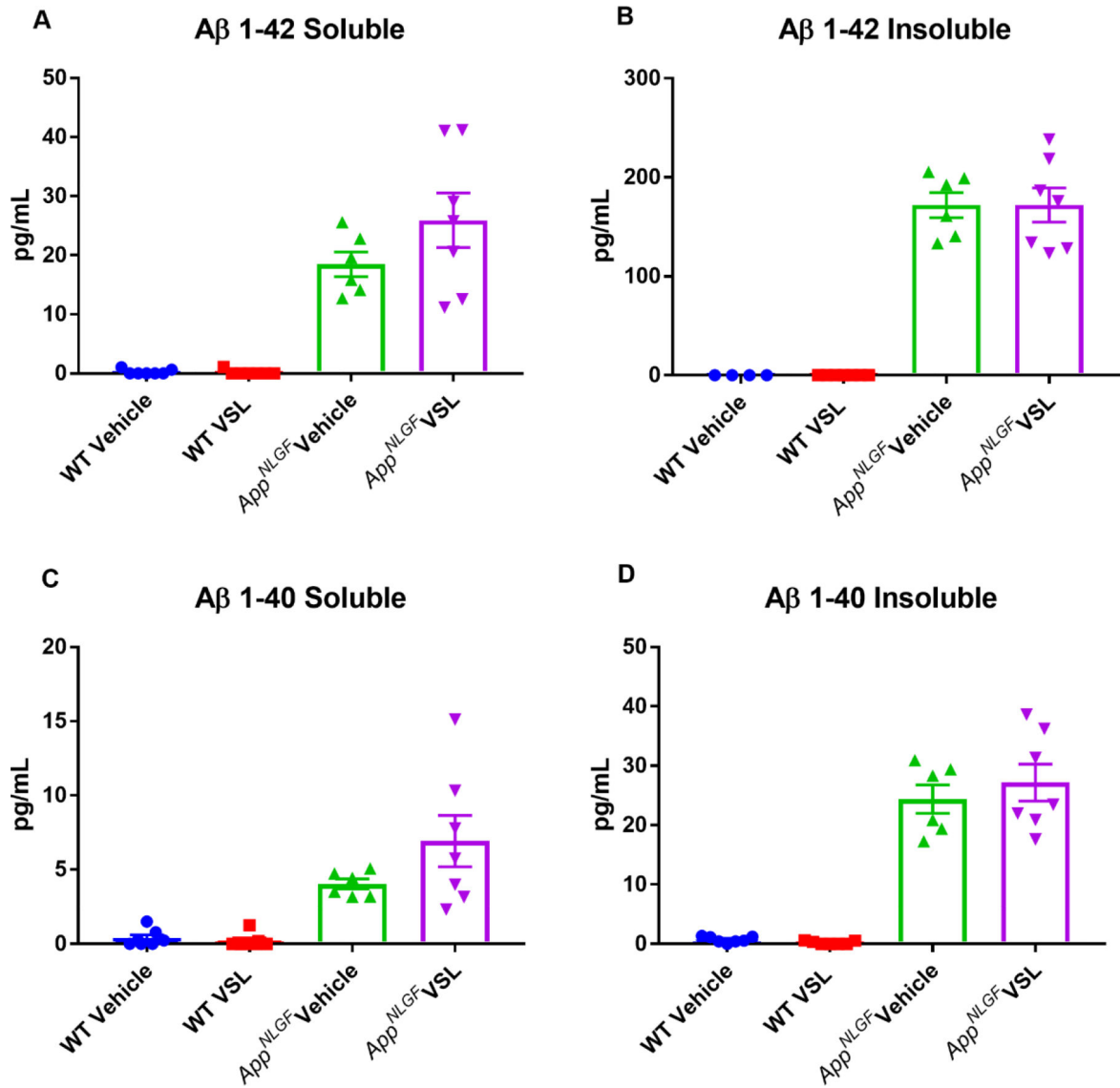


Fig. 9. Effect of VSL#3 dietary supplementation on hippocampal Aβ levels. Female C57BL/6 wild type and *App^{NL-G-F}* mice were provided normal drinking water or water supplemented with probiotic, VSL#3, *ad libitum* from 6–8 months of age. Hippocampi were isolated, lysed, and levels of Aβ 1–40 and Aβ 1–42, both soluble and insoluble, were quantified by ELISA. Seven animals per group were examined and the data are presented as mean ± SEM.

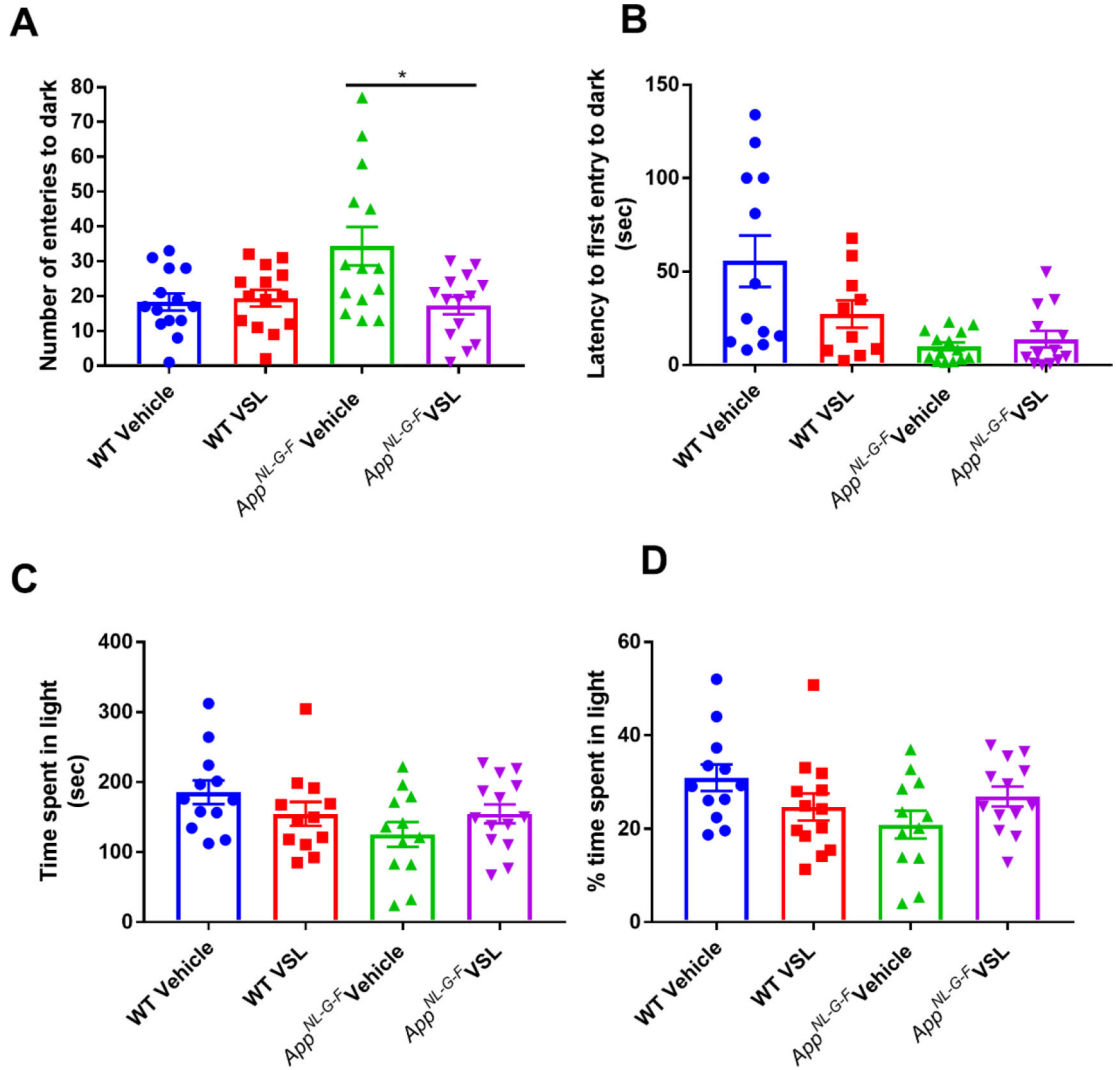


Fig. 10. Effect of VSL#3 supplementation on anxiety in C57BL/6 (WT) and *App^{NL-G-F}* mice. Female C57BL/6 wild type and *App^{NL-G-F}* mice were provided normal drinking water or water supplemented with probiotic, VSL#3, *ad libitum* from 6–8 months of age. All mice were subjected to light-dark test after 8 weeks of treatment and (A) total number of entries into the dark compartment, (B) latency of first entry into the dark compartment, (C) time spent in the light compartment, and (D) the percentage of time spent in the light were determined. Data are represented as the mean ± SEM (n=14). Significant differences between vehicle and VSL#3 treated animals in each genotype were determined by t-test; * p<0.05.